ELSEVIER

Coordination Chemistry Reviews
197 (2000) 95–124

COORDINATION CHEMISTRY REVIEWS

www.elsevier.com/locate/ccr

Molecules with hydride or alkyl ligands and including d^0 transition metal centers: problem cases for the simple VSEPR model

G. Sean McGrady [a,*], Anthony J. Downs [b]

[a] *Department of Chemistry, King's College London, Strand, London WC2R 2LS, UK*
[b] *Inorganic Chemistry Laboratory, University of Oxford, South Parks Road, Oxford OX1 3QR, UK*

Received 18 February 1999; accepted 8 July 1999

Contents

* Corresponding author. Tel.: +44-171-8481212; fax: +44-171-8482810.
E-mail address: sean.mcgrady@kcl.ac.uk (G.S. McGrady)

PII: S0010-8545(99)00198-8

Abstract

Application of the simple VSEPR model to hydride and alkyl derivatives of Main Group and transition elements is considered, and successes and failures of the model are outlined. A survey is presented of the difficulties inherent in the precise location of hydrogen atoms in molecules, and of techniques developed to surmount these problems. Consideration is given to a selection of Main Group and d^0 transition metal molecules which do not comply with the expectations of the model. These include halides such as MF_2 (M = Ca, Sr or Ba), permethyl complexes like WMe_6, and mixed-ligand species such as Me_2TiCl_2 and Me_3ReO_2. Theoretical attempts to account for this behavior, including extensions to the simple VSEPR model, are described. The phenomenon of 'agostic' M···H interaction is considered in the context of d^0 transition metal complexes. Whilst rationalization of the phenomenon is beyond the remit of the VSEPR approach, a molecular orbital model is shown to give more insight than does an earlier valence-bond approach in explaining the salient features of the interaction.

Keywords: Hydride; Alkyl; Transition metals

"This world's no blot for us,
Nor blank; it means intensely, and means good:
To find its meaning is my meat and drink."

Robert Browning, *Fra Lippo Lippi*, 1.313

1. Introduction

1.1. The VSEPR model

Of the models developed to rationalize chemical properties few can have combined alluring simplicity with predictive fidelity more successfully than has the valence shell electron pair repulsion (VSEPR) model. The seminal idea that molecular geometry is determined by the arrangement of electron pairs in the valence shell was first articulated by Sidgwick and Powell nearly 60 years ago [1]. From this sprang the basic tenets of the VSEPR Theory, which were spelt out by Nyholm and Ron Gillespie more than 40 years ago [2]. Since then Gillespie has been the chief architect and exponent of the Theory, through subsequent review articles [3,4] and books [5,6] elaborating on its use for the prediction and rationalization of molecular geometry.

Controversy continues to follow the central assumption that electron–electron repulsion dominates the choice of molecular geometry [7,8]. In fact, the electronic energy of a molecule can be divided into four contributions: (i) the kinetic energy of the electrons, E_{ke}, (ii) the electron–nuclear attraction, E_{en}, (iii) the nuclear–nuclear repulsion, E_{nn}, and (iv) the electron–electron repulsion, E_{ee}. Ab initio calcula-

tions carried out on CH_4 [7b] show that the relative magnitudes of these terms follow the order

$$E_{en} > E_{ke} > E_{ee} > E_{nn}$$

The electron–nuclear attraction, which is the primary term in molecular orbital treatments (wherein electron–electron repulsion is ignored to a first approximation), makes the largest contribution, E_{en} being more than four times the magnitude of E_{ee}. However, none of the terms can be discounted; even the smallest, E_{nn}, is more than 20 times the total binding energy of the CH_4 molecule. Ab initio calculations do give some support to the primacy of electron–electron repulsion as a stereochemical influence [7b]. Thus, the calculated increase in energy when NH_3 exchanges its stable pyramidal configuration for a planar one is dominated by the increased repulsion between the lone pair on the one hand and the three bond pairs on the other [9]. However, the calculation overestimates by at least two orders of magnitude the actual increase in total energy so that the change in E_{ee} must be largely offset by changes in the other terms. Whether we are right to follow the VSEPR hypothesis that it is the only term to be considered is a matter of doubt.

What is not in doubt is that the VSEPR model, as developed and refined by Gillespie, provides an intelligible and remarkably reliable rationale for the shape of many molecules. The basic ideas have been reformulated to some extent: for example, the space occupied by an electron pair is now termed its 'domain', the shape and spatial demands of which vary from molecule to molecule [4,6]. Without being based on any orbital model, the resulting domains give a very approximate description of the electron distribution in a molecule that is based on the role of the Pauli principle in dictating the electron density distribution. The physical basis of the model has also gained credibility from more recent ab initio studies that have led to the calculation of accurate electron density distributions of several molecules: the very approximate descriptions suggested by the model are consistent not only with these distributions but also with the Laplacians of the relevant electron density [6,10]. The Laplacians are noteworthy for signalling the presence of local charge concentrations of electron density with all the properties of size and location that are imputed to the electron-pair domains of the VSEPR model.

In its simplest form the VSEPR approach is best adapted to deal with molecules centered on Main Group elements. Here it is reasonable to suppose that the core underlying the valence shell of the central atom is spherical and therefore exercises no influence on the geometry. By contrast, open-shell molecules where the central atom is a transition metal are more problematic since the partially occupied d-shell is liable to produce a core with an ellipsoidal rather than a spherical shape [4,6]. In the present review we are concerned not with systems of this sort but with molecules containing metal atoms that apparently possess spherical cores [4,6]. The case histories to be described deal for the most part with molecules containing two to six electron pairs in the valence shell of the central atom. That atom is in some cases a Main Group element but more often a transition metal in a formal oxidation state implying that it has a d^0 configuration. According to the VSEPR model, the idealized geometries to be expected are, then, as follows:

Number of domains	Arrangement
2	Linear array
3	Trigonal planar array
4	Tetrahedron
5	Trigonal bipyramid
6	Octahedron

When the domains in a given molecule are rendered inequivalent by the presence of different substituents, we anticipate departures from the geometric ideal to reflect the presumptions that multiple-bond domains take up more room in the valence shell than do single-bond domains, and that the domain associated with a single bond becomes more demanding of space as the electronegativity of the substituent decreases.

In Section 2 we will show that metal atoms possessing what appears to be a stereochemically inactive electron core can, nevertheless, form molecules whose ground-state geometries depart from VSEPR-based preconceptions, sometimes quite radically, sometimes more subtly. Prominent among the examples to be considered are d^0 transition metal compounds such as WMe_6 and Me_2TiCl_2, in which the metal is typically coordinated to one or more alkyl ligands. At current levels of sophistication, quantum-chemical calculations are able to reproduce remarkably well the observed geometries and spectroscopic properties of the molecules, but without necessarily shedding much light on just why one structure is different from another. One simple explanation is to be found in the notion of core polarization which needs to be applied as an additional constraint on normal VSEPR rules [4,6]. It is instructive, however, also to take stock of other simple yet plausible explanations of the facts.

If Section 2 treats problem cases that can be accommodated, up to a point, by VSEPR arguments, Section 3 deals with some structural peculiarities that lie largely beyond the reach of the model. Here the scene changes to geometric perturbations induced by complexation of some d^0 alkyl-transition metal compounds. Now it appears that the changes arise from the development of supplementary bonding involving a so-called 'agostic' interaction between the metal center and a saturated CH_n group of an alkyl ligand already tethered to the metal via a conventional σ-bond. We examine the facts established specifically for the parent compound $EtTiCl_3$ and for its phosphine complex $[EtTiCl_3(dmpe)]$, where dmpe = $Me_2PCH_2CH_2PMe_2$, on the basis of detailed X-ray diffraction and spectroscopic measurements; in the light of these and of the results of density functional theory (DFT) calculations, we gain a clearer picture of just how the secondary bonding arises and what it entails. In that electron delocalization is now the principal author of structural change, agostic systems really represent a stage too far for the VSEPR model, founded as it is on localized electron-pair domains.

1.2. Hydride and alkyl derivatives of Main Group and transition elements

The molecules with which we are concerned are mostly centered on d^0 transition metal atoms; derivatives of s- and p-block elements feature less often and mainly for comparative purposes. The ligands to be treated will be F, Cl, O, H, Me, or Et. Of especial interest are the last three. Each is a one-electron ligand with no significant potential for π-type interactions, and which may function as a medium σ-donor to a medium-strong σ-acceptor. A valence orbital energy more nearly comparable with that of the metal center results in M–H or M–C bonds that are much less polar than, say, M–F or M–Cl bonds. Beyond this, however, it is difficult to ascribe any general ligand characteristics to either hydrogen or alkyl (R) groups on account of their polarizability, the nature of the M–H and M–C bonds varying with the nature not only of M but also of any other ligands that may be linked to M.

The structures of molecules containing hydride or alkyl ligands provided some of the early triumphs of rationalization for the VSEPR model. For example, the methyl-substituted fluorophosphoranes, Me_nPF_{5-n} ($n = 1–3$), were shown by GED studies carried out by Bartell et al. [11] to have heavy-atom frameworks each approximating more or less closely to a trigonal bipyramid with the methyl substituents confined exclusively to the equatorial belt (see Fig. 1). Such a pattern is wholly consistent with arguments to the effect that, for reasons of ligand electronegativity, the domain of the P–C bonding electron pair is more demanding of space in the valence shell of the central phosphorus atom than is the domain associated with the P–F bonding electron pair [2–6]. The same holds true for the P–H, as compared with the P–F, bonding electron pair in the hydridofluorophosphoranes, H_nPF_{5-n} ($n = 1–3$), the geometries of which [12] emulate those of the analogous methyl derivatives but, as illustrated in Fig. 1, with methyl giving place to hydrogen in the equatorial sites. Successive replacement of equatorial fluorine by methyl or hydrogen leads, as expected, to a regular and significant increase in the axial P–F bond lengths. Although the bond angles in the equatorial plane imply

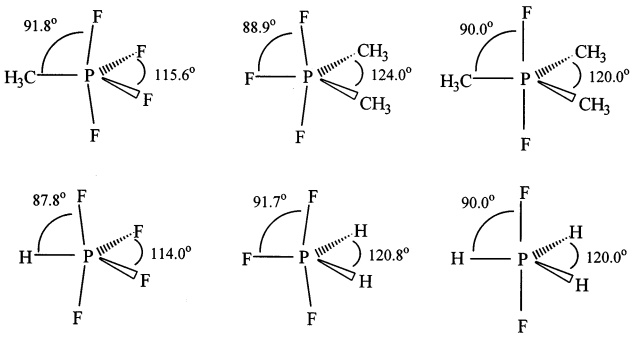

Fig. 1. Molecular structures and skeletal geometries of Me_nPF_{5-n} and H_nPF_{5-n} ($n = 1–3$) in the gas phase as determined by electron diffraction or rovibrational spectroscopy [11,12].

that the P–C or P–H bonding electrons take up more space in the valence shell of the phosphorus than do the P–F bonding electrons, the F_{ax}–P–F_{ax} unit of HPF_4 and H_2PF_3 is, if anything, bent *towards* and not away from the equatorial P–H bonds [12]. Details like these should remind us that there are recesses in the chemistry of Main Group elements that the simple VSEPR model is unable to reach.

Hydrogen and alkyl groups have the capacity also to act as bridges between two or more coordination centers, as in species like $H_2Ga(\mu^2\text{-}H)_2GaH_2$ and $Me_2Al(\mu^2\text{-}Me)_2AlMe_2$. The geometries of the resulting molecules are consistent in reflecting the reduced electron density associated with an 'electron deficient' bridge bond which gives a less expansive domain than do the electrons responsible for a more conventional terminal bond. However, the delocalization implicit in the bridging structures necessarily takes away much of the predictive power of the VSEPR model — as opposed to its power to explain a posteriori. From bridge bonds of this sort it need not take a giant stride to reach hydrogen bonds, both conventional and unconventional [13], as well as other forms of 'secondary' interaction which are capable of functioning in either inter- or intra-molecular modes. Weak these interactions may be, with energies typically in the region of 10–50 kJ mol^{-1}, but they may be quite strong enough to tip the balance between a pyramidal or planar NH_3-like molecule, or to change the conformation of an ethane derivative C_2H_5X. Not to be discounted, therefore, is the potential stereochemical influence of secondary H···M interactions, where M can be one of a variety of elements, including H itself.

1.3. Techniques for the precise location of hydrogen atoms in molecules

The structures of alkylmetal compounds form one of the recurring themes of this review, and although our primary concern is limited in some cases to the heavy-atom skeleton of the molecule, the location and detailed characterization of the C–H bonds of the alkyl ligand have sometimes been crucial to establishing the facts of the case. In view of the practical difficulties that have to be overcome, it is appropriate to outline briefly the measures that can be taken to quantify as accurately as possible the dimensions of the coordinated alkyl ligand.

1.3.1. Diffraction measurements on crystalline solids

The structural scene is dominated, as usual, by X-ray diffraction studies of single crystals. However, this technique has its limitations originating mainly in the low scattering cross-section of hydrogen and the difficulties inherent in locating hydrogen atoms in the vicinity of metal atoms of much higher atomic number. To make matters worse, the vibrational amplitudes associated with H atoms at room temperature are frequently large, with the result that the scattering from these atoms is not only weak but more than usually diffuse. Moreover, estimates of the lengths of bonds to hydrogen fall short of the values determined by spectroscopic or other means, typically by about 0.1 Å, as a result of the non-spherical distribution of electron density about the hydrogen nucleus.

Some of these problems can be significantly alleviated by the combination of good crystal quality, low crystal temperature, and the use of CCD or image plate technology [14]. For more accurate location of the hydrogen atoms, however, neutron diffraction must be the method of choice. Neutron scattering cross-sections for hydrogen and, better still, deuterium offer an altogether superior prospect of locating H atoms precisely, and without any systematic shortening of the bonds in which they are engaged. On the basis of appropriate neutron-diffraction studies and the improved capability of modern X-ray facilities, charge density studies are coming increasingly to be mapped [15] in a way that now promises to illuminate much more clearly some of the intricacies of chemical bonding.

1.3.2. Structures of gaseous molecules

The gas phase offers the only medium for structural analysis effectively to eliminate intermolecular forces as a factor liable to perturb the equilibrium structure of the free molecule. Unfortunately, though, studies of gaseous molecules are too often frustrated by problems of thermal stability, involatility, or molecular complexity. High-resolution spectroscopic techniques probing the rotational transitions are limited in practice to all but the simplest molecules; the hydridofluorophosphorane H_3PF_2 [12] is a rare example of a molecule whose structure has been accurately determined by a detailed analysis of its rovibrational spectrum. Even precise measurements of this sort cannot disguise the uniquely low atomic mass of hydrogen and the small contribution that it necessarily makes to the momental ellipsoid. In the event, electron diffraction has been the mainstay of structural studies involving gaseous molecules. To the electron diffraction pattern of a molecule, however, there are distinct limitations: it does not discriminate well between interatomic distances that are comparable in magnitude, and the relatively weak scattering of bound or unbound M···H atom pairs again tends to impair accurate location of the hydrogen atoms. From the pattern alone it is rarely possible to extract good estimates of all the structural and vibrational parameters that determine the molecular scattering. The best response in these circumstances is to carry out a combined analysis incorporating the geometric and vibrational information carried not only by the electron diffraction pattern, but also by the rotational constants and an appropriate force field, where these are known or can at least be meaningfully approximated. A further development described recently is the so-called SARACEN method [16] whereby parameters which cannot be refined freely are made subject to restraints derived from a graded series of ab initio calculations (q.v.).

1.3.3. Studies of vibrational spectra

The frequencies of the C–H stretching fundamentals are a sensitive function of the dimensions and other properties of organic groups, although any direct correlation must be of an empirical nature. By partial deuteration to give CHD_{n-1} units, McKean and his colleagues have been able largely to eliminate the complications of Fermi resonance and determine 'isolated' C–H stretching frequencies, ν^{is}CH, which correlate remarkably well with r_0(C–H), H–C–H bond angles, and

D_0°(C–H), and so appear to provide a sensitive index to these and other properties [17]. On the evidence of recent studies, this approach is applicable to organometallic species like $RTiCl_3$ (R = Me or Et) no less than conventional organic molecules [18].

1.3.4. Theoretical methods

Current studies of molecular structure depend in no small part on the input of modern quantum chemical methods. High level ab initio calculations admitting the use of relatively elaborate basis sets, as well as making due allowance for refinements like configuration interaction and relativistic corrections, are now widely accessible. Where comparisons can be made, calculations of this sort typically yield molecular dimensions, energies, vibrational wavenumbers and intensities in infrared absorption or Raman scattering, and chemical shifts that reproduce closely the experimental findings, and sometimes *improve upon* those findings. The SARACEN method [16] is a striking example of the synergy that can develop between experiment and theory, with the ab initio calculations guiding, but not dictating, the analysis of the experimental results. As will become clear in Section 3, density functional theory (DFT) calculations [19] have been equally influential in unravelling some of the structural peculiarities that appear to result from secondary interactions between a C–H bond of an alkyl ligand and a d^0 transition metal center. However, what these sophisticated calculations may gain in predictive precision is often at the expense of an intelligible indication of the causes of a particular structural phenomenon. In this respect, they are a supplement to, not a substitute for, VSEPR and other simple models.

2. Geometries of alkyls and halides of the Main Group and d^0 transition elements: non-compliance with the simple VSEPR model

2.1. Some problematic halide derivatives

Limitations in the applicability of VSEPR Theory in its simplest form to certain alkaline-earth dihalide molecules came to be appreciated at an early stage in the development of the model. This particular episode has been complicated by difficulties in establishing unambiguously the facts of the case. Electric deflection studies, carried out on molecular beams in the early 1960's certainly implied that some MX_2 molecules (M = Ca, Sr, or Ba; X = F or Cl) have non-linear geometries, with X–M–X angles less than 150° [20]. With due allowance for the possible effects of aggregation, matrix perturbation or 'shrinkage', these conclusions have gained support from subsequent investigations by matrix isolation [21] and gas electron diffraction (GED) [22]. By the same token, though, the dihalides of beryllium and magnesium emerge as linear molecules.

Subsequent studies by Gillespie and Bader explored more subtle effects in a series of oxide halide molecules built on d^0 transition metal atoms [4–6,23]. Hence they noted that molecules such as $V(O)F_3$ [24] and $Cr(O)_2F_2$ [25] conform to the dictates

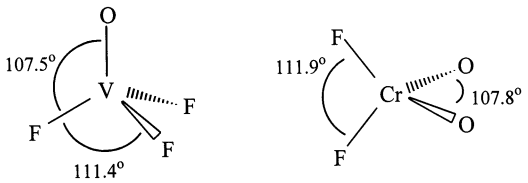

Fig. 2. Molecular structures and skeletal geometries of $V(O)F_3$ and $Cr(O)_2F_2$ in the gas phase as determined by electron diffraction [24,25].

of the simple VSEPR model in terms of *gross* skeletal geometries, but that the *angles* subtended at the central metal atom by the M=O and M–F bonds run counter to the normal conventions of that model. As Fig. 2 shows, the electrons making up the M=O 'double' bonds appear sterically more compact than do the electrons making up the M–F 'single' bonds. Other anomalous features are also revealed, for example in the *cis*-dioxo structure favored by the anion $[Cr(O)_2F_4]^{2-}$ [26].

2.2. Structures of alkyl derivatives of d^0 transition elements: the facts

2.2.1. Neutral and anionic permethyl compounds, $[MMe_n]^{m-}$

In 1989 Morse and Girolami reported the first structure to be determined for a d^0 transition metal alkyl of this sort, viz. $[ZrMe_6]^{2-}$ [27]. X-ray diffraction studies of a single crystal of the compound $[Li(tmed)]_2[ZrMe_6]$ revealed an anion possessing not octahedral but *trigonal prismatic* geometry, the heavy-atom skeleton conforming to D_{3h} symmetry; the cations bridge between two methyl groups lying along a trigonal edge but were not considered to have a significant bearing on the geometry of the anion. The following year saw the publication by Haaland et al. [28] of the structure determined for the gaseous WMe_6 molecule on the basis of GED measurements. Here too the results implied a trigonal prismatic structure, the observed diffraction pattern being quite incompatible with a WC_6 skeleton possessing regular octahedral geometry. In a subsequent GED study, the penta-coordinated d^0 molecule $TaMe_5$ was shown to have a TaC_5 skeleton in the form not of a trigonal bipyramid (cf. $SbMe_5$) but of a square-based pyramid with C_{4v} symmetry [29]. Although this result is not at first sight incompatible with the prognosis of the VSEPR model (bearing in mind, for example, that the square-based pyramid is also the form adopted by a few molecules formally containing five electron pairs in the valence shell of a Main Group element, e.g. $SbPh_5$ [30]), the skeletal bond angles leave little doubt that electron pair repulsion forces alone do not dictate the finer details of the ground-state structure.

Compounds like WMe_6 pose a formidable challenge to the experimentalist by virtue of their chemical reactivity and propensity to detonate without warning [31]. In a technical *tour de force*, Pfennig and Seppelt have developed techniques for growing and manipulating crystals of these materials at temperatures below −80°C; hence they succeeded in preparing needle-shaped single crystals of both

WMe_6 and its d^1 analog $ReMe_6$ that diffracted very well at -163°C [32]. The unit cell of WMe_6 contains two crystallographically different molecules that are very much alike and differ only in their packing. No crystallographic symmetry is enforced on either molecule. Surprisingly, though, the skeleton of the WMe_6 molecule is found to have not the trigonal prismatic (D_{3h}) structure deduced from the GED experiment [28], but a less regular geometry which can be derived from the D_{3h} one by opening up one trigonal face and closing the other. The skeleton thus possesses C_{3v} symmetry with three W–C bonds subtending C–W–C angles of 75.4 to 78.2 ± 0.4° somewhat longer than the other three that subtend C–W–C angles of 93.3 to 96.9 ± 0.5° (Fig. 3). The vibrationally averaged structure of this non-rigid molecule would have D_{3h} symmetry and is not necessarily incompatible with the measured GED pattern which has been analyzed to date only in terms of a more or less 'rigid' model. By contrast with WMe_6, $ReMe_6$ has an ReC_6 framework altogether closer to the trigonal prismatic ideal (see Fig. 3), although it still emulates WMe_6 in the sense if not the degree of its distortion from D_{3h} symmetry. In a subsequent report, Seppelt et al. described the structures of $[NbMe_6]^-$ and $[TaMe_6]^-$ [33]. These too each show a distortion from ideal trigonal prismatic symmetry in a manner similar to, but much less pronounced than, that displayed by WMe_6; as with $[ZrMe_6]^{2-}$ [27], the structure may be influenced by bridging interactions with Li cations.

More recently, the structures of the anions $[WMe_7]^-$ and $[ReMe_8]^{2-}$ have been characterized by crystallographic studies of the salts [Li(base)][WMe_7] (base = Et_2O or Me_3N) and $[Li(OEt_2)]_2[ReMe_8]$ at low temperatures [34]. Hence it emerges that $[WMe_7]^-$ is built like a monocapped octahedron (with C_{3v} symmetry) and $[ReMe_8]^{2-}$ like a regular square antiprism (with D_{4d} symmetry). The anomalies of the parent hexamethyl compounds find no echo here, for the structures of the anions are unremarkable, finding ample precedent in species like $[MF_7]^-$ (M = Mo or W), $[ThMe_7]^{3-}$, and $[XF_8]^{2-}$ (X = Re, W, I or Xe). For coordination numbers

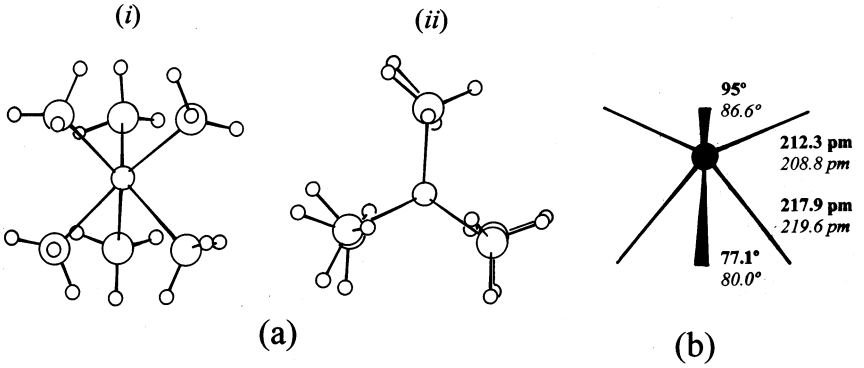

Fig. 3. (a) Molecular structures of WMe_6 and $ReMe_6$ as determined by single crystal X-ray diffraction at low temperature viewed (i) perpendicular to the threefold molecular axis and (ii) down this axis. (b) Schematic representation of the C_{3v} distorted trigonal prism found for WMe_6 and $ReMe_6$. Averaged bond lengths and angles are shown for WMe_6 (bold) and $ReMe_6$ (italic) [32].

greater than six, the stereochemistry appears to be controlled primarily by inter-ligand contacts; accordingly, any reversion to what may seem like VSEPR-type behavior is probably illusory.

2.2.2. Mixed ligand derivatives incorporating methyl and chloro or oxo ligands

The situation in a molecule incorporating two different types of π-bonding ligand has already been introduced in the form of species like $Cr(O)_2F_2$ [25]. If the coordination sphere is made up of a mixture of σ-only ligands and ligands with the capacity to enter into π-type interactions, the gross features of the structure may be unsurprising, but the devil is in the details. Such is the case with the methylmetal chlorides $MeTiCl_3$ [35], Me_2TiCl_2 [36], Me_2NbCl_3 [37], and Me_3NbCl_2 [37], and the oxides $MeReO_3$ [38] and Me_3ReO_2 [39], the structures of which have been determined by GED measurements.

The titanium compounds have been investigated in some detail. On the evidence of the GED patterns, the structures of the gaseous molecules $MeTiCl_3$ and Me_2TiCl_2 are as depicted in Fig. 4. The most striking feature is not the gross skeletal geometry, which clearly approximates to the tetrahedral array to be expected of a valence shell containing four pairs of electrons, but the bond angles. The bonds to the more electronegative substituents (Cl) subtend the *greater* angle at the Ti atom. This is quite the opposite of the behavior shown by analogous derivatives of Main Group elements, such as Me_nSiCl_{4-n} [40], where the corresponding bonds subtend the *smaller* angle; it thus contravenes the normal VSEPR rules regarding the rôle of ligand electronegativity [2–6]. No satisfactory explanation is to be found by invoking a degree of Ti–Cl π-bonding since the experience gained from transition metal oxide halides like $Cr(O)_2F_2$ [23–25] is that bonds normally supposed to involve appreciable π-bonding appear to take up less and not more room in the valence shell of the transition metal atom. In any case, the results of valence-shell photoelectron spectroscopy measurements on $MeTiCl_3$ suggest that $Cl \rightarrow Ti$ π-donation is modest [41]. Nor is the answer to be found in inter-ligand repulsion for there is actually *more* space in the coordination sphere of Ti(IV) than in that of Si(IV).

The structures of the niobium compounds Me_2NbCl_3 and Me_3NbCl_2 (Fig. 4) pose more questions than they answer [37]. Each is formally based on trigonal bipyramidal coordination of the metal; the methyl ligands occupy exclusively equatorial sites imparting skeletal symmetries of D_{3h} to Me_3NbCl_2 and of C_{2v} to Me_2NbCl_3. Following the example of the methyltitanium systems described above, the bond angles in the equatorial belt of Me_2NbCl_3 appear to manifest the greater spatial demands of Nb–Cl compared with Nb–Me bonding electrons, the C–Nb–C angle being compressed to 115(2)°. If this is the correct reading of the situation, the structure is then at odds with the occupation in both Me_2NbCl_3 and Me_3NbCl_2 of the axial positions not by Me but by Cl ligands, since the VSEPR model and its associated concept of 'apicophilicity' [42] view these sites as subtending a *smaller* angle at the central atom. Further peculiarities are evident also in the Cl_{ax}–Nb–Cl_{ax} unit of Me_2NbCl_3, which is significantly distorted, the Nb–Cl_{ax} bonds being bent away from the unique Nb–Cl_{eq} one so as to give a Cl_{ax}–Nb–Cl_{eq} bond angle of

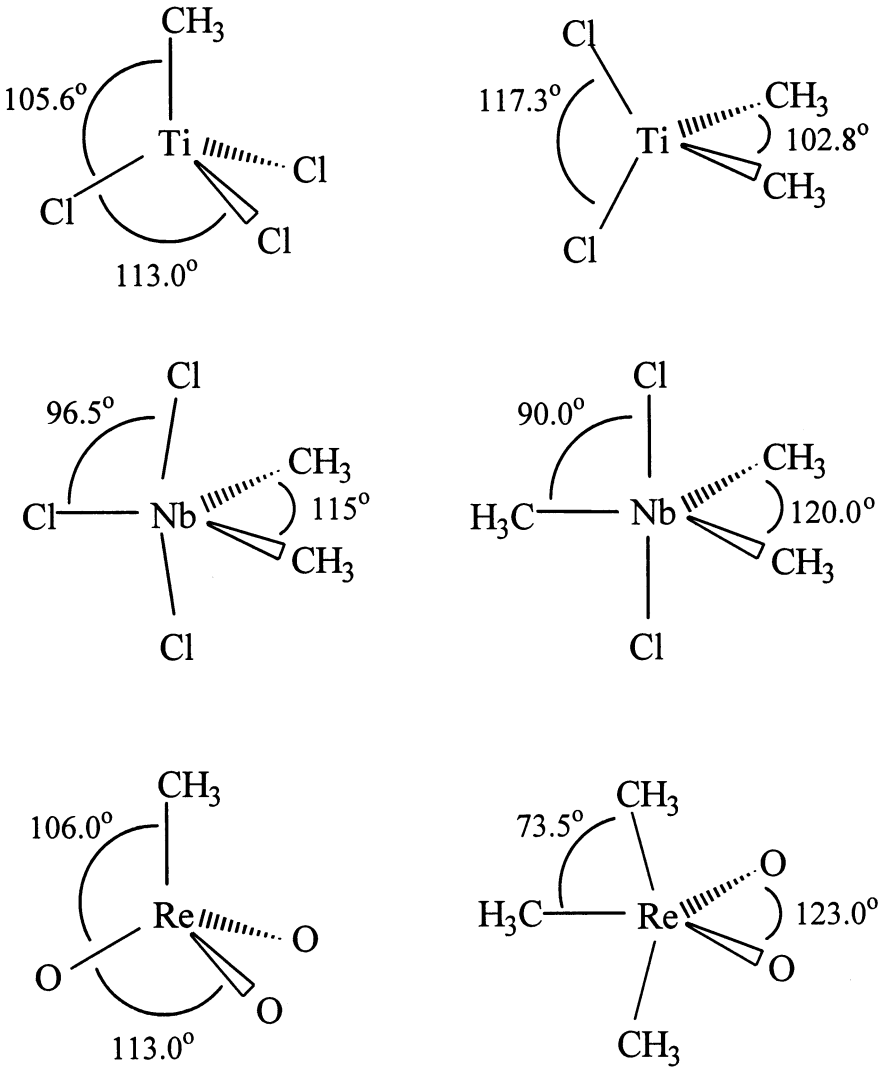

Fig. 4. Molecular structures and skeletal geometries of $MeTiCl_3$, Me_2TiCl_2, Me_2NbCl_3, Me_3NbCl_2, $MeReO_3$ and Me_3ReO_2 in the gas phase as determined by electron diffraction [35–39].

96.5(3)° [37]. Indeed, the skeletal geometry of Me_2NbCl_3 may justifiably be viewed as arising from the distortion not of a trigonal bipyramidal but of a *square-based pyramidal* arrangement of five bond domains (q.v.).

The methylrhenium(VII) oxides $MeReO_3$ and Me_3ReO_2 involve competition between two ligands at opposite ends of the π-bonding spectrum, i.e. σ-only methyl and the strongly π-interacting oxo groups. Indeed, valence-shell photoelectron and ^{17}O-NMR studies imply that the Re–O linkages in $MeReO_3$ enjoy a bond order in excess of 2 [38]. The structures of $MeReO_3$ [38] and Me_3ReO_2 [39], depicted also in

Fig. 4, show no clear correlation between the numbers of each ligand and the bond angles they subtend at Re. Thus, if $MeReO_3$ is formally derived from a tetrahedral array and Me_3ReO_2 from a trigonal bipyramidal one with the π-bonding oxo ligands in equatorial sites, then the O–Re–O angle of 113.0(3)° in the monomethyl derivative is larger than the tetrahedral value, and the corresponding angle of 123.0(20)° in the trimethyl derivative is also wider than the trigonal value (120°). These multiple bond domains behave as might be expected in each case, although with such strongly π-bound Re–O linkages, orbital overlap considerations are likely to play a significant role, and the observed angles probably reflect electron-nucleus forces more than electron-electron or steric repulsions. The Re–Me moieties in Me_3ReO_2, however, exhibit peculiarities (i) in the magnitude of the C_{ax}–Re–C_{eq} bond angle which at 73.5(11)° is highly compressed from the VSEPR ideal, and (ii) in the disposition of the axial methyl groups, whose local C_{3v} axis is not coincident with the Re–C bond vector [39]. This last feature is beyond the scope of the present review, but the distortion of the C_3ReO_2 skeleton follows a pattern opposite to that discussed above for Me_2NbCl_3, suggesting that the structure of Me_3ReO_2 may have its origins in an edge-bridged tetrahedral, rather than a trigonal bipyramidal, framework. Along with the structure deduced for $TaMe_5$ [30] (see Section 2.2.1), the present findings prompt the view that the trigonal bipyramid may be less pervasive in penta-coordinated d^0 transition-metal systems than in analogous derivatives of the Main Group elements [31].

2.3. Interpretation

The non-linear nature of some alkaline earth dihalide molecules posed the first serious challenge to the VSEPR approach. In an extension to the model, Gillespie proposed that the electron core of heavier atoms from the Main Groups and transition blocks may be susceptible to polarization by electron pairs in the valence shell [4–6,23]. Such polarization results in charge localizations which then compete for space with the charge concentrations arising from lone pairs and bonding pairs of electrons in the valence shell: the consequence is a departure from the idealized geometry forecast on the basis of normal VSEPR arguments. Recent developments in quantum chemical methods, and most notably in density functional theory (DFT) [19], admit the realistic calculation of charge densities in molecules containing light or medium-sized atoms. This facility was exploited by Gillespie to explore the equilibrium structures of the alkaline-earth dihalides. Here he was aided by the pioneering work of Bader, whose 'Atoms in Molecules' theory [43] is becoming widely recognized as a most powerful analytical tool for teasing out problems of structure and bonding. Gillespie and Bader were thus able to provide the first direct experimental evidence validating core polarization as the author of the bent geometries assumed by some dihalide molecules of the heavier alkaline-earth metals. Thus, topological analysis of the charge density in the CaF_2 molecule clearly showed local charge concentrations to exist in the core of the Ca atom [44]. The two bonding electron pairs associated with the F–Ca–F skeleton seek then to avoid these concentrations by adopting a non-linear disposition.

The anomalous bond angles in mixed oxide halide derivatives of d^0 transition metals, e.g. $Cr(O)_2F_2$ [25], responded to a similar approach, analysis of the charge density in the core of the metal atom providing a rationalization of the apparent aberrations. The more covalent metal–oxygen bonds are perceived to induce a diametrically opposed polarization of the metal atom core which transcends that induced by the more polar metal–halogen bonds (Fig. 5). It follows that the VSEPR-favored structure 'relaxes' into a configuration of lower energy once

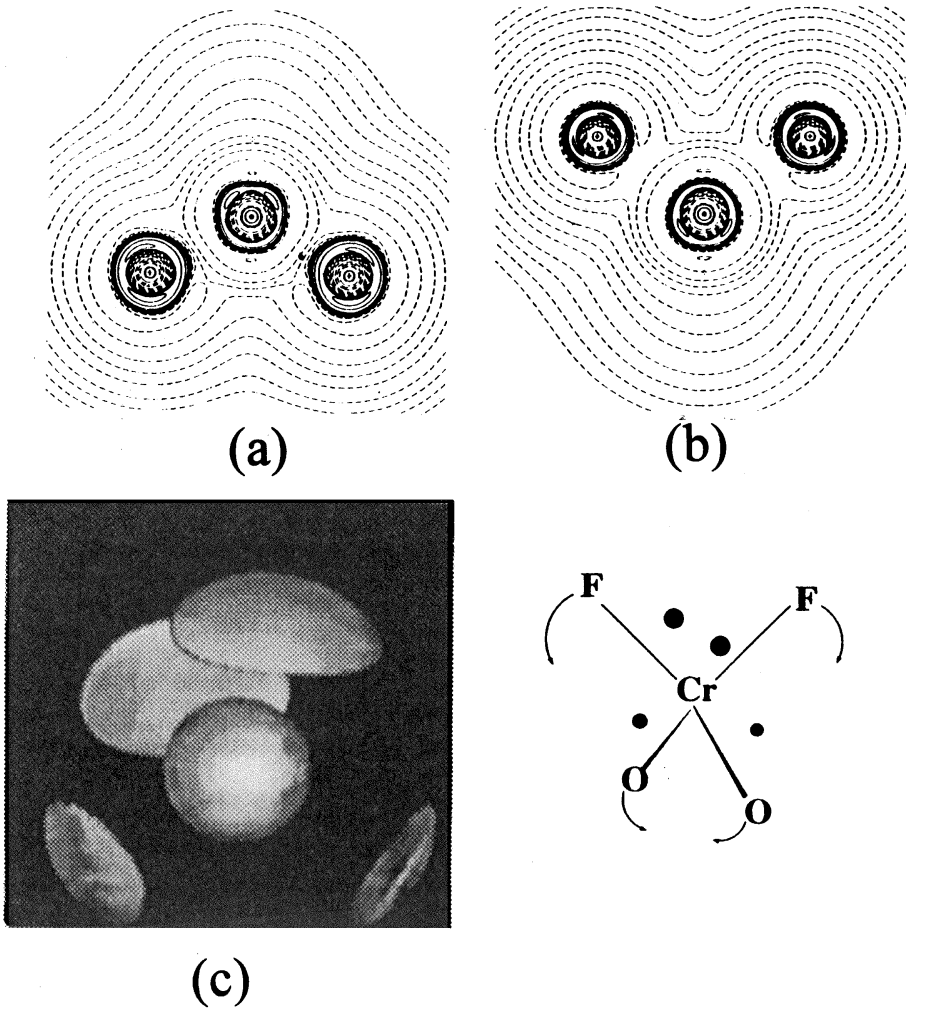

Fig. 5. Contour and envelope maps of the Laplacian of the total electron density for $Cr(O)_2F_2$ (a) in the O–Cr–O plane, showing two opposed ligand charge concentrations (CCs) in the Cr core; and (b) in the F–Cr–F plane, showing the other two ligand CCs that form an overall tetrahedral arrangement of charge concentrations. (c) Envelope map illustrating the tetrahedral arrangement of CCs and the larger size of those opposed to the oxide ligands. Reproduced with permission from Ref. [25].

provision is made for these charge concentrations, along with the normal interactions between bonding pairs of electrons.

The structure and bonding of molecular transition-metal compounds incorporating only σ-bound ligands exercised the minds of many theoreticians in the 1970s. On the basis of Extended Hückel calculations, research groups led by Hoffmann [45], and later Eisenstein [46], published seminal papers predicting that d^0 systems such as WH_6 would not adopt the VSEPR-preferred octahedral geometry in their equilibrium ground states. As with the halide systems already discussed, access to more sophisticated quantum chemical methods by the mid-1980s prompted the reinvestigation of this and related problems by DFT and other methodologies. Calculations carried out by Tang [47], Kaupp [48] and others have verified the predictions first entered by Hoffmann et al. [45]: ML_6 species such as WH_6 and WMe_6, where there is no contribution from metal-ligand π-bonding, are *inherently non-octahedral in their electronic ground states*.

A similar conclusion may also be drawn in a more qualitative way by consideration of the frontier MOs of a σ-bonded ML_6 system initially prescribed to have octahedral symmetry and appeal to second-order Jahn Teller arguments [49]. Main Group species of this type, as exemplified by $TeMe_6$, are made stable with respect to distortion to lower symmetry by the large energy gap separating the HOMO and LUMO. In a similar vein, a transition metal species like WF_6 also retains octahedral symmetry as the π-donor F ligands serve to stabilize the t_{1u} HOMO. In the case of WH_6 or WMe_6, however, the presence of low-lying vacant orbitals of metal t_{2g} character means that no such stabilization can be achieved. Furthermore, the relatively electropositive H or CH_3 ligands have the effect of raising the energy of the t_{1u} HOMO to a level close to the metal-based t_{2g} LUMO. Although HOMO-LUMO mixing is strictly forbidden in O_h symmetry, the action of an appropriate normal mode results in a lowering of symmetry to either D_{3h} or C_{3v}, under which a common irreducible representation is spanned by the HOMO and LUMO. Mixing of these two previously orthogonal sets of orbitals must then follow, with the resultant stabilization of the HOMO through the admixture of metal d functions into what is a primarily ligand-based orbital set, as depicted in Fig. 6. For d^0 systems such as WMe_6, the C_{3v} structure is favored over D_{3h} on electronic grounds; occupation of the a′ orbital in the d^1 complex $ReMe_6$ drives the geometry back towards D_{3h} [32]. This geometry may also be favored for d^0 $[ZrMe_6]^{2-}$ on account of the negative charge which is located largely on the ligands, or additionally on account of the pronounced cation-anion interactions observed for this complex in the solid state [27].

Landis et al. have explored the bonding of transition metal alkyls and hydrides through an extension and generalization of the valence-bond concepts first proposed by Pauling in the 1930s [50]. The metal is considered to rely for its bonding mainly on hybrid orbitals of sd^n character. Some of the conclusions are surprising: for example, systems in which the metal possesses more than 12 valence electrons are formally regarded as 'hypervalent', the excess of electrons being accommodated in three-center, four-electron bonds. Not only does this simple approach reproduce reliably the unusual geometric features displayed by homoleptic transition metal

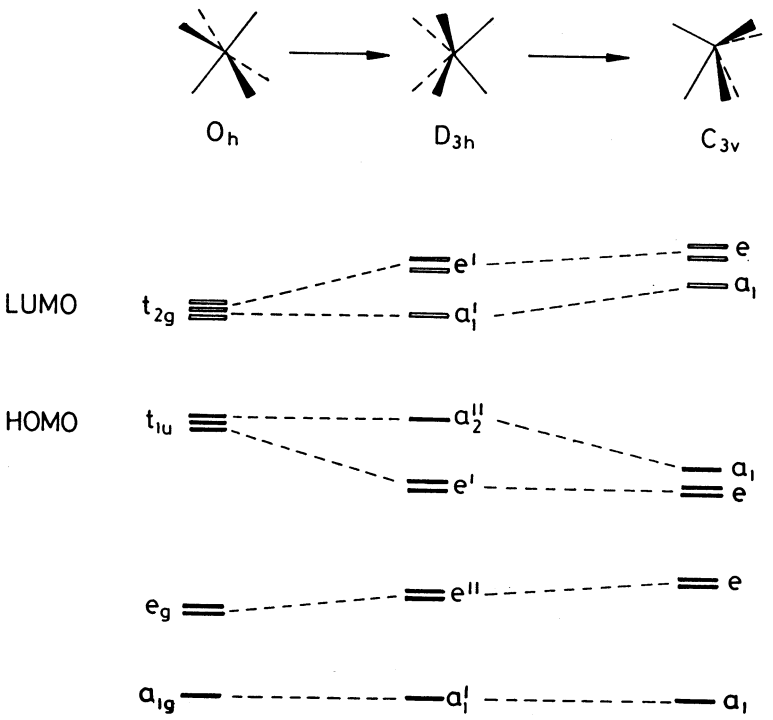

Fig. 6. Qualitative molecular orbital diagram for d^0 MMe_6 complexes. Occupation of the empty a_1 orbital in the C_{3v} structure will drive the geometry back towards D_{3h} [32].

alkyls, it affords results that are consistent with more detailed analyses drawing on high-level quantum chemical calculations. It has the added attraction, through the invocation of three-center, four-electron MH_2 units in electron-rich polyhydrides, that it is able naturally to accommodate dihydrogen as a ligand [51].

On the other hand, Gillespie's notion of core polarization [4–6,23] offers a simple alternative way of explaining the non-conformist structures of molecules like WMe_6. The charge concentration of core electron density induced by, and lying diametrically opposed to, each M–C or M–H bond disfavors the disposition of the bonding electron pairs associated with such bonds at 180° to each other. For a penta-coordinated system, the square-based pyramid has the advantage over the trigonal bipyramid that it need contain no diametrically opposed bonding pairs of electrons.

The structures determined experimentally for $MeTiCl_3$ and Me_2TiCl_2 provide an apparent contradiction of Bent's Rule which, as formulated for Main Group systems, states that 'atomic s-character concentrates in the orbitals directed towards the more electropositive ligands' [52]. Bent's Rule works admirably within the p-block, and can be used to rationalize bond angles in molecules such as Me_2SiCl_2, as well as general trends revealed by sets of molecules such as CH_4, NH_3, OH_2 and NH_3/OH_2 vs. NF_3/OF_2. It owes its success in these cases to the situation wherein

the central atom, E, draws on its valence *n*s and *n*p orbitals for the bonds it forms to the ligands (Fig. 6). The higher-energy *n*p electrons, being more easily oxidized, concentrate preferentially in bonds to more electronegative ligands. For this reason E–F bonds have more p-character and accordingly are spatially less demanding than are E–C or E–H bonds.

Frenking et al. invoked an analogous scheme to describe the bonding in molecules having a d^0 transition metal center, with the difference that the brunt of the bonding is now borne by the valence *n*s and $(n-1)$d orbitals, so far as the central atom is concerned [53]. In this case the *n*s orbital lies at *higher* energy than does the $(n-1)$d manifold, and so the orbitals directed towards the more electronegative ligands should take on *more* and not less s-character. For the Me_2TiCl_2 molecule, for example, it follows that the bonds to the more electronegative Cl substituents may be expected to subtend an angle *greater than* 109.5° at the metal center, in keeping with the apparently anomalous dimensions of this molecule (Fig. 7).

A valence-bond approach to the same problem meets with less success [36]. Construction of a set of sd^3 hybrid orbitals on the Ti atom of Me_2TiCl_2 suggests that relaxation of the C_2TiCl_2 skeleton from a regular tetrahedron to the geometry determined by experiment should lead to a concentration of s-character not in the Ti–Cl but in the Ti–C bonds. The conclusions are therefore at odds with those derived from Frenking's simple model. Attempts to resolve the conflict by analysis of the wavefunctions of Me_2TiCl_2 have to date been less than conclusive. It is not obvious then that either of these simple models is able convincingly to explain the skeletal geometries of Me_2TiCl_2 and related molecules.

The Gillespie remedy involving polarization of the transition metal core [4–6,23] avoids any such impasse. With reference once again to the Me_2TiCl_2 molecule, the more covalent Ti–C bond induces in the Ti core a diametrically opposed charge

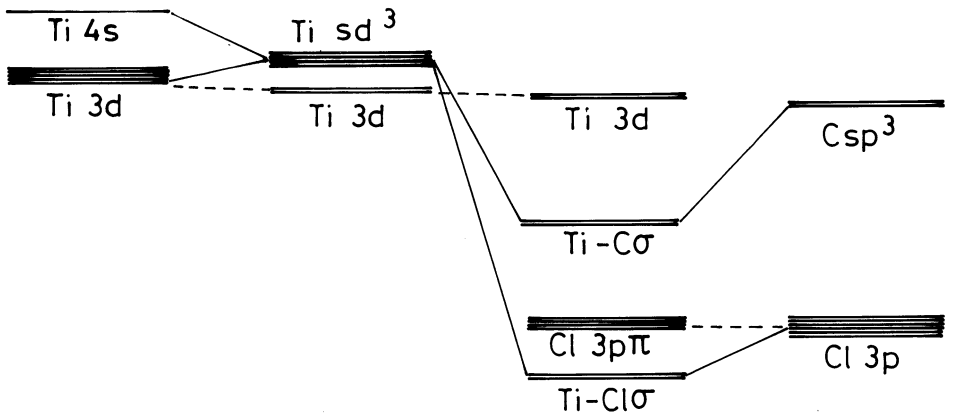

Fig. 7. Qualitative molecular orbital scheme for Me_2TiCl_2. Construction of sd^3 hybrid orbitals on Ti results in Ti–Cl bonding orbitals containing greater than 25% s character and Ti–C orbitals with correspondingly enhanced d character [53]. See Ref. [36] for an alternative approach to the problem.

concentration which is greater than that built up *trans* to the more ionic Ti–Cl bond. The additional interactions thus created provide a natural driving force tending to open out the Cl–Ti–Cl and close up the C–Ti–C angle of the C_2TiCl_2 skeleton.

3. Secondary M···H interactions in transition metal alkyls

3.1. 'Agostic' C–H···M interactions: their nature, occurrence, effects and relevance

The strength, non-polar nature and low polarizability of C–C and C–H bonds, allied to the chemical saturation of coordinated alkyl groups, cause us generally to consider them as being chemically inert. However, a growing body of crystallographic and spectroscopic evidence led to the realization in the early 1980s that alkyl ligands can in certain circumstances coordinate to a transition metal M in an η^2-fashion [54]. Where reliable structures have been determined for these systems, it appears that the primary M–C bond is supplemented by a significant secondary interaction involving an unusually short C–H···M contact. Such a situation has been characterized for C–H groups disposed α, β, γ or even further along the alkyl chain with respect to M, and is now commonly described as 'agostic', a term first coined by Green to describe this particular phenomenon [54]. Examination of the wider scene has revealed two generic types of agostic interaction: (i) 'open' interactions in which the coordinated C–H bond is part of a polyene ligand bound to the metal; and (ii) 'closed' interactions where a C–H bond of a saturated alkyl ligand is drawn towards the metal. This review is concerned solely with 'closed' interactions.

Recognition of this hitherto unperceived bond-type has wrought a profound change of understanding as to the chemical behavior of saturated organic ligands, with vital implications for several important processes. Among these are two large-scale commercial operations, viz. hydroformylation and Ziegler Natta polymerization [55,56]. More generally, agostic bonding is now perceived as highly relevant to the activation of C–H bonds in coordinated alkyl groups [57], and finds obvious parallels in the area of hydrosilylation, in which an Si–H bond coordinates in an η^2-manner to a metal center in an *inter*molecular interaction [58]. A central reaction of transition metal alkyls is β-elimination, a reversible process by which the alkyl is converted into the corresponding metal alkene hydride. In that the reaction proceeds by C–H bond fission and formation of an M–H bond, a C–H···M agostic situation must represent a stage on the reaction coordinate defining β-elimination. What has revolutionized our thinking, however, is the notion that this stage can actually be the *ground state* under appropriate conditions. With so much evidently at stake, there is a compelling need to elucidate the true nature, origins and consequences of agostic bonding.

Initial recognition of the phenomenon can be traced to studies of the adducts $RTiCl_3(dmpe)$ (R = Me or Et; dmpe = $Me_2PCH_2CH_2PMe_2$) [54c]. Characterization of single crystals of the methyl compound by X-ray and neutron diffraction shows

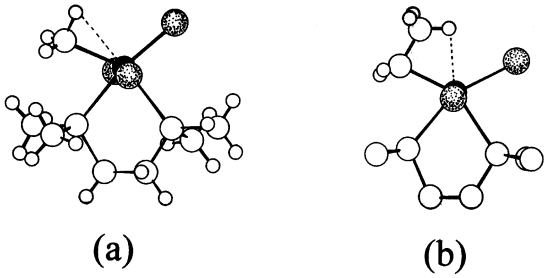

Fig. 8. Molecular structures of $RTiCl_3(dmpe)$ [R = Me (a), Et (b)] as determined by single crystal X-ray (a, b) and neutron (a) diffraction. In each case the Ti–R geometry is highly distorted, with close approach of a C–H bond towards the Ti center, suggesting a Ti···H–C interaction [54c].

the geometry of the Ti–CH_3 unit to be highly distorted, as illustrated in Fig. 8. The CH_3 group is canted with respect to the Ti–C vector so that one hydrogen comes suggestively close to the Ti center, giving a Ti–C–H angle of 93.5°. In the ethyl compound the C_2H_5 group is bent to close down the Ti–C–C angle from the customary range of 108–126° to about 86°, thereby bringing one of the CH_3 hydrogen atoms close to the metal. Neither structure gives grounds for believing that intermolecular forces play any part in influencing the extraordinary disposition of the alkyl groups. Hence these complexes came to be established as prototypes of α- and β-agostic interactions, respectively. Once the idea had gained currency, hundreds of structures have been claimed subsequently, with varying degrees of conviction, to bear the signs of agostic interactions.

Green et al. considered the abnormal structures to result from the electron-deficient nature of the Ti center [54]. Reductive elimination — a primary reaction in organometallic chemistry — may be conceived for $[MeTiCl_3(dmpe)]$ and $[EtTiCl_3(dmpe)]$, leading to $[CH_2Ti(H)Cl_3(dmpe)]$ and $[(\eta^2\text{-}C_2H_4)Ti(H)Cl_3(dmpe)]$, respectively. The highly electron-deficient nature of the metal in each of the parent complexes [with a valence electron (VE) count of only 12] provides a driving force for such a rearrangement. In each case, however, the metal center has to adopt a d^2 configuration if the reactions are to proceed to completion; the d^0 configuration of Ti(IV) denies the metal the electron pair it needs to support the ligand environment of the elimination products. For this reason, the distorted structures found for the Ti–CH_3 and Ti–CH_2CH_3 moieties in the dmpe complexes have been interpreted [54] as arrested stages on the reaction coordinate leading to elimination. The C–H···Ti agostic unit was postulated as being held together by a 3-center, 2-electron bond, with donation of electron density occurring from the C–H bonding orbital into a vacant orbital confined mainly to the metal, implying a bridging hydrogen atom bonded to both C and Ti, with a concomitant degree of metal hydride character.

Such a model implies that the development of an agostic interaction is impelled mainly by the electroneutrality principle and the need to relieve the electron deficiency of the metal center, with an increase in the VE count towards the

saturation value of 18. In summary, then, four desiderata can be identified as being expected to favor agostic bonding [54]:

- an unsaturated transition metal center M with a VE count of less than 18;
- the possession by M of a vacant acceptor orbital of appropriate energy and disposition;
- coordination of the metal center by fewer than the maximum number of ligands it is capable of supporting; and
- an increase in the positive charge carried by M.

The model has much to commend it. For one thing, it is able successfully to accommodate agostic interactions within the wider framework of concepts developed to explain the structure and reactivity of organometallic complexes [54]. Its Achilles' heel, however, is its poor predictive power. Thus, the factors listed may represent necessary or desirable *prerequisites*, but experience has shown that they are in no way *sufficient* to provide a reliable prognosis of just where agostic interactions will or will not be found. Indeed, the majority of organotransition metal compounds that formally satisfy these conditions show little or no evidence of agostic behavior. In the next section we elaborate on this point with specific reference to ethyltrichlorotitanium, $EtTiCl_3$, and its dmpe complex, and draw on the results of recent experimental and quantum-chemical studies in an attempt to seek a clearer understanding of the agostic phenomenon.

3.2. Some detailed studies of ethyltrichlorotitanium, $EtTiCl_3$, and its response to complexation by bidentate phosphine ligands

The structure of $EtTiCl_3$(dmpe), as determined by X-ray diffraction of a single crystal, was reported in 1986 [54c], with results that played a key rôle in the recognition and rationale of agostic interactions. The complex was described as exhibiting a curiously distorted Ti–CH_2–CH_3 fragment (Fig. 8), in which a C–H bond of the β-carbon appears to be attracted to the highly electron deficient Ti center with its VE count of only 12; the coordination of a C–H bond manifests perhaps an attempt to alleviate this situation. Although the complex is built around a Ti center that is formally hexa-coordinated the ligand environment shows no obvious steric resistance to incorporation of the ethyl ligand in an η^2-manner.

The structure of the parent $EtTiCl_3$ molecule in the gas phase was determined by electron diffraction by Haaland et al. only in 1998; simultaneously the structure of $EtTiCl_3$(dmpe) was scrutinized closely on the basis of more detailed and accurate X-ray studies carried out on single crystals at low temperature [59]. Compared with its dmpe adduct, $EtTiCl_3$ features a metal center with a lower VE count and coordination number, as well as an increased positive charge. If the characteristics outlined in Section 3.1 are any guide, therefore, it offers a stronger case for agostic bonding than does the dmpe adduct, and might be expected accordingly to develop even more robust secondary interactions. Beyond the urge to put these arguments to the test, the studies were also motivated by the determination to rule out impurities (like $TiCl_4$) as a factor liable to compromise experimental findings [54c]. The combination of reactivity, thermal fragility and difficulty of freeing from $TiCl_4$

makes $EtTiCl_3$ a daunting practical proposition; it is impossible to eliminate every trace of decomposition product (whether from β-elimination or from reactions with vestiges of moisture or other agents harbored by the surfaces exposed to the compound). Only by adopting rigorous high-vacuum techniques similar to those deployed for the synthesis and manipulation of base-free gallium hydrides [60] have the hazards of contamination been minimized.

The reality of the parent $EtTiCl_3$ molecule came as something of a surprise. The structure of the gaseous molecule as determined by GED measurements embodies a 'normal' $Ti–CH_2–CH_3$ geometry, with a staggered configuration about the C–C bond and a Ti–C–C angle of 116.6(11)° [59]. Indeed, the magnitude of this angle suggests that the $C_\beta H_3$ group is not so much attracted to, as *repelled by*, the Ti center. In other respects, the skeletal geometry follows closely the precedents set by $MeTiCl_3$ [34] and Me_2TiCl_2 [36] (see Section 2.2.2).

The effect of varying the Ti–C–C angle on the total energy of $EtTiCl_3$ was explored by DFT calculations [59], with the remarkable results depicted in Fig. 9. These showed the potential energy surface characterizing Ti–C–C bending to be uncommonly flat. The shape of the surface reflects in part the marked polarity of the Ti–C bond, but the calculations revealed another factor adding to the shallowness of the relevant potential well: at a Ti–C–C angle of about 100°, rotation of the $C_\beta H_3$ group occurs to eclipse the Ti–C bond and bring one C–H bond in close proximity to the metal, creating an eclipsed conformer which displays a potential energy surface even flatter than that of its staggered counterpart.

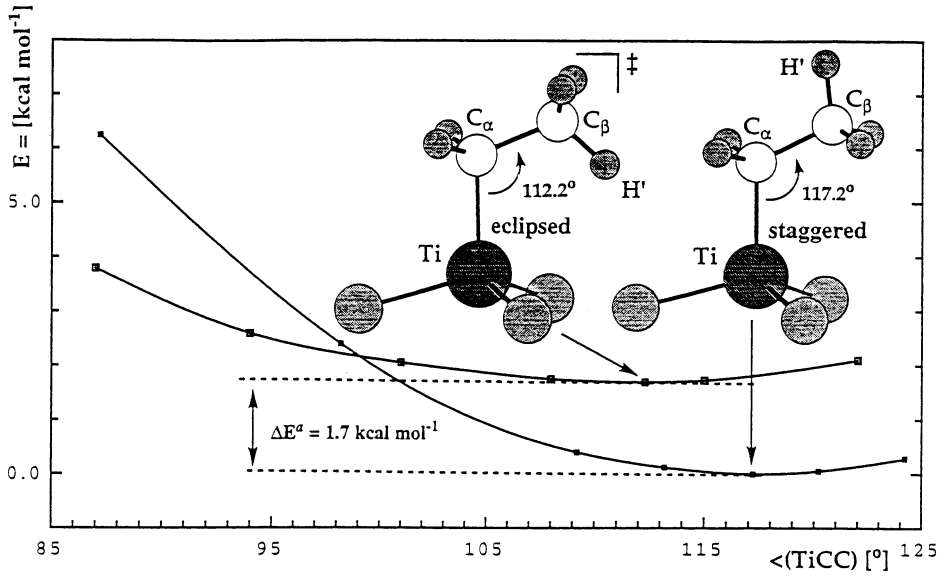

Fig. 9. Variation of the total energy with Ti–C–C angle in $EtTiCl_3$ for eclipsed and staggered conformers. Primes indicate the location of an atom either in (′) or out of (″) the C_s symmetry plane of the molecule. Reproduced with permission from Ref. [61].

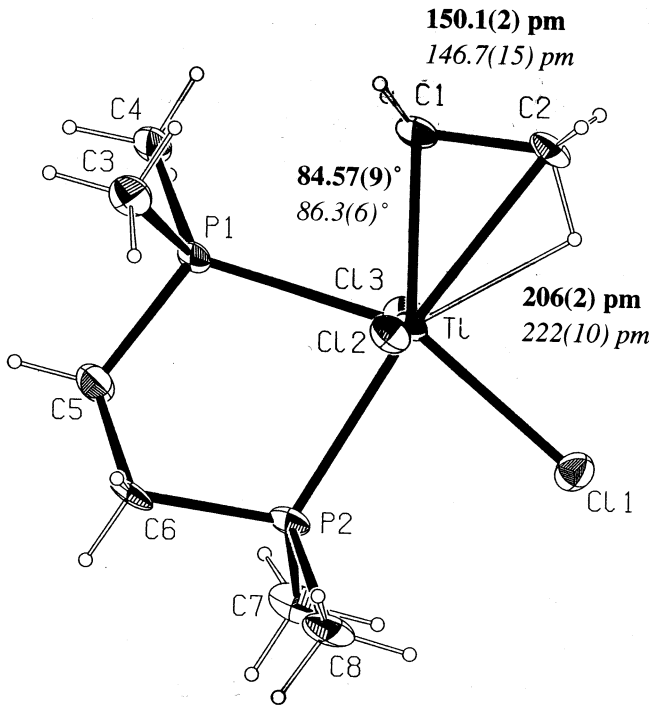

Fig. 10. Molecular structure of $EtTiCl_3$(dmpe) determined by single crystal X-ray diffraction at 105 K. Salient structural parameters are indicated (bold), along with those from an earlier determination [54c] (italic). Reproduced with permission from Ref. [59].

The equilibrium structure of $EtTiCl_3$ (Fig. 9) is characterized by a non-bonded $C_\beta \cdots Cl''$ distance of 383 pm [60], just larger than the sum of the van der Waals' radii for CH_3 and Cl (375 pm). A major reason for the surprisingly large Ti–C–C angle is that the Cl–Ti–Cl angles, at about 113°, are themselves larger than tetrahedral – a peculiarity of such mixed-ligand systems discussed in Section 2.2.2. Calculations in which the Ti–C–C angle was reduced to 87° [the value found experimentally for $EtTiCl_3$(dmpe)] showed this non-bonded distance to be reduced to 343 pm, thereby affording a measure of the significant steric resistance to such a process [61]. The combination of the flat potential surface and the energetics of the two conformers of $EtTiCl_3$ reflects a contest between two opposing forces: (i) β-agostic attraction, which favors an eclipsed structure and small Ti–C–C angle, and (ii) inter-ligand repulsion, which favors a staggered structure and large Ti–C–C angle. $EtTiCl_3$ may thus be regarded as a molecule where a β-agostic interaction is *incipient*.

The crystal structure of the diphosphine complex $EtTiCl_3$(dmpe) at low temperature [59] leaves no doubt about the essential authenticity of the original report [54c]: the geometry of the EtTi fragment is now conspicuously different, the $TiCH_2CH_3$ moiety assuming an *eclipsed* conformation and featuring an acute Ti–C–C valence angle of 84.57(9)°. The Ti atom and the equatorial atoms Cl(1), P(1), P(2), C(1) and

C(2) are nearly coplanar, whereas the two Ti–Cl(2) and Ti–Cl(3) bonds are approximately perpendicular to the equatorial plane (see Fig. 10). The coordination geometry may therefore be described as distorted octahedral, with the entire ethyl group occupying one coordination site. Here the signs of a β-agostic interaction are unmistakable.

But why should the agostic interaction be only incipient in the tetra-coordinated $EtTiCl_3$ molecule yet openly developed in the hexa-coordinated dmpe adduct? Examination of the structural data for both molecules reveals that there is actually *more* space for the ethyl group to rearrange in the adduct than in the base-free molecule. Complexation *opens out* the coordination sphere and *renders it more pliable*; as a consequence the closest $C_\beta H_3 \cdots Cl$ contact in the $EtTiCl_3$ fragment of the adduct with its eclipsed $TiCH_2CH_3$ group is increased from 343 to 358 pm [59,61]. This finding serves as a salutory reminder that steric effects cannot be assumed to increase as a simple function of coordination number; each case must evidently be considered on its merits.

The calculations help to clarify the complex rôle played in agostic interactions by the ligand environment. The electronic nature of the interaction has also been explored by Haaland et al. [61], again by recourse to DFT methods. Hence it has been possible to devise a molecular orbital model for the interaction that contrasts with the valence bond model described in Section 3.1, and also gives rise to conclusions somewhat at odds with those suggested by the lore associated with that model.

The HOMO of $EtTiCl_3$, depicted in Fig. 11, represents the Ti–C_α bonding orbital, but with two further important features: it is delocalized significantly onto C_β and its appended H atoms, and its construction from the d_z2 orbital on Ti provides a component of the HOMO in the plane normal to the Ti–C_α vector. The

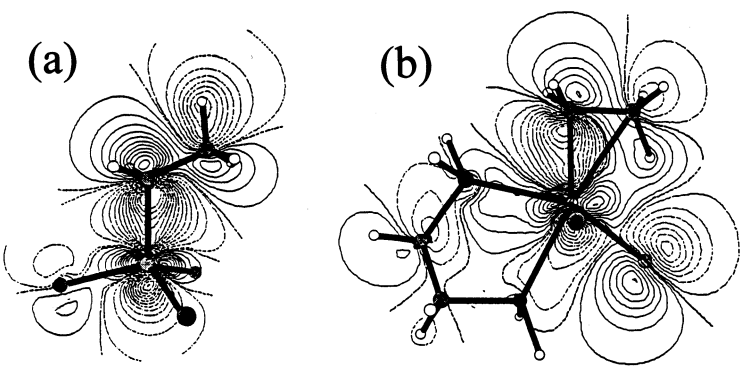

Fig. 11. Contour maps of the HOMO of (a) $EtTiCl_3$ and (b) $EtTiCl_3$(dmpe). In each case the HOMO consists of the Ti–C_α bonding orbital, which exhibits substantial delocalization onto C_β and its appended H atoms. The extra flexibility and space in the coordination sphere of the adduct permits the ethyl ligand to cant and establish a bonding interaction between the metal and a C_β–H fragment. Reproduced with permission from Ref. [59].

constant electron density contours show the HOMO to be antibonding with respect to any Ti–C_β interaction in the base-free molecule.

The HOMO in the dmpe adduct, also depicted in Fig. 11, has essentially the same composition and nature as in $EtTiCl_3$, but there is a subtle difference: the extra space and pliability created by addition of the diphosphine ligand permits the ethyl group to cant. Accordingly, C_β and one of its appended H atoms establish a bonding interaction with the component derived from the torus of the d_z2 orbital on Ti. This rearrangement of the HOMO results in its delocalization, with a stabilization amounting to some 27 kJ mol^{-1} relative to the corresponding anagostic system in which the Ti–C–C angle is constrained at 112°. The major contribution to the agostic stabilization appears to be $C_\beta\cdots$Ti bonding. By contrast, the $C_\beta H_3$ group appears on the evidence of the calculation and of spectroscopic investigation to enjoy 'in place' rotation, with no more than ca. 10% of the estimated stabilization energy attributable to the Ti···H component of the interaction. Stabilization of the Ti–C bond (the HOMO) appears therefore to be the major driving force in the development of the β-agostic interaction. Accordingly, the phenomenon is best described as essentially a two-electron process involving only a *single* orbital on the metal.

These conclusions were investigated by appealing to a variety of structural and spectroscopic techniques in order to interrogate $EtTiCl_3$ and its dmpe complex. In a study of several isotopomers, McGrady et al. [62] explored the vibrational properties of the ethyl group in $EtTiCl_3$ and the way these changed on complexation. The results proved to be more or less consistent with the model outlined above. Of particular note were the implications for the nature of the C_β–H···Ti unit which accorded much more closely with the requirements of the molecular orbital than with those of the valence bond approach. The vibrational properties of the EtTi moiety argue that attachment of the C_β–H unit to the metal occurs largely through the carbon atom, with a perturbation in the frequencies of, but not in the normal coordinates describing, the C_β–H modes. The same study also succeeded in measuring the first value of an 'isolated' C–H stretching mode (see Section 1.3) for an agostic system; at 2585 cm^{-1}, this turns out to be some 200 cm^{-1} lower than any other ν^{is}CH frequency reported hitherto. Undoubtedly there is significant perturbation of the unique C_β–H bond that points towards the metal, but not to the extent of detectable chemical activation, at least to judge by preliminary chemical tests. Coordination of $EtTiCl_3$ by dmpe results not only in a marked decrease in frequency of one of the $\nu(C_\beta H)$ modes, but also in a simultaneous *increase* in frequency of the $\nu(C_\alpha H)$ modes associated with the methylene portion of the ethyl ligand. Here the vibrational properties intimate a strengthening of the C–H bonds, as well as a widening of the H–C–H angle.

NMR studies of solutions have exploited the method developed by Shapley et al. [63] in seeking evidence for an isotopic perturbation of resonance (IPR) for the CH_2CH_2D isotopomer of $EtTiCl_3$(dmpe) [61]. That no such IPR was apparent can be understood if there is a minimal difference of chemical shift between the agostic and terminal H nuclei attached to C_β, thereby negating the basis of the Shapley experiment and at the same time confuting the notion of a significant degree of hydride character for the agostic hydrogen nucleus. Indeed, the revised view of the hydrogen atom in the C–H···M unit offered by the molecular orbital model

provides a timely explanation of the comparative unprofitability of the Shapley method in probing agostic interactions at large [64].

Scherer et al. have carried out high resolution X-ray diffraction studies on a single crystal of $EtTiCl_3$(dmpe) at -168°C with the aim of determining the electron density distribution in the complex [65]. The charge densities determined experimentally on the basis of a standard multipole model were combined with those calculated by DFT methods in a topological analysis depending on the Bader 'Atoms in Molecules' approach [44]. Despite the demonstrable presence of a β-agostic interaction, the total electron density reveals no significant accumulation of charge between the metal and the $C_\beta H_\beta$ unit. With little or no evidence for direct Ti···H bonding, then, the results add weight to the molecular orbital model. The charge densities emphasize the polar nature of the Ti–C_α bond (reflecting the electropositive nature of Ti) which, as noted previously, is a primary cause of the peculiar flexibility that distinguishes the Ti–CH_2–CH_3 skeleton. An additional feature brought to light by the gradient vector map $\nabla\rho(r)$ is a significant curvature in the Ti–C_α bond path, the bond critical point being displaced outwards some 6 pm from the $TiC_\alpha C_\beta H_\beta$ assembly. Not only does this finding comply with the notion that the Ti–C_α bonding electrons are actually delocalized over the entire Ti–C_2H_5 fragment, it may well be a distinctive hallmark of a β-agostic interaction.

In a parallel study, Haaland et al. [61] have carried out a series of DFT calculations on model ethyl–transition metal systems related to $EtTiCl_3$ in an attempt to elucidate the relative importance of the factors listed in Section 3.1 in promoting a β-agostic interaction. The method of attack was to compare the energy of the optimized ground state structure with that of a system in which the M–C–C angle was constrained to be 112°, while all the other geometric parameters were optimized. For tri-coordinated metals, the systems showed a proclivity to agostic behavior that declines in the order:

$$[EtTiCl_2]^+ \gg EtScCl_2 > EtTiCl_2$$

With no significant steric resistance to the change of geometry, this ordering reflects the importance of a positive charge on the metal center in stabilizing the interaction, to which the d^0 configuration of the neutral scandium system is evidently better predisposed than is the d^1 configuration of its titanium analog. On the other hand, extension of this analysis to tetra-coordinated ethyl-metal compounds exposed some surprising features. Here the order of agostic stabilization was found to be:

$$EtNbCl_3 > EtVCl_3 > EtZrCl_3 > [EtVCl_3]^+ > EtTiCl_3$$

As expected, complexes of the larger second-row metals Zr and Nb are more likely to show agostic behavior than are complexes centered on their first-row congeners Ti and V. Quite unexpected, however, is the lowly position of the cationic vanadium species, which is distinctly less prone to agostic bonding than is its neutral parent $EtVCl_3$. On the strength of both a lower valence electron count and the Coulombic advantage of a positive charge, the cation would be expected to outstrip the neutral molecule. What we have not bargained for is revealed, though,

by the DFT analysis, namely that the tetra-coordinated species are markedly less flexible than the tri-coordinated ones. Closer examination of the 'extra' d^1 electron in $EtVCl_3$ shows it to occupy an MO derived largely from the d_{xy} orbital on V, but which displays significant V–Cl antibonding character (Fig. 12). The electron serves therefore to render less rigid the ligand environment around the vanadium atom and to facilitate the distortions required for canting of the ethyl group and establishing a $C_\beta H_3 \cdots M$ interaction.

This situation then finds parallels with the effects of complexation on $EtTiCl_3$. Increasing the number of ligands around the metal from three to four appears generally to result in a stiffening of the ligand framework. A β-agostic interaction is an inherently weak bond with an interaction energy typically in the order of 20 kJ mol^{-1}. To accommodate the interaction is likely in practice to require loosening of the metal environment, whether by inclusion of extra d electrons on the metal or by complexation with a donor ligand. On the evidence available at the present time, this feature carries more weight than do the perceived disadvantages of reduced positive charge, increased valence electron count, or enlarged coordination shell that attend the changes.

In summary, rigorous structural and spectroscopic investigations, in conjunction with quantum-chemical calculations, on judiciously selected model systems have produced a new model for describing β-agostic interactions in ethyl derivatives of early transition metals. This model differs from the earlier valence-bond description in certain important respects, most notably in its treatment of the nature and properties of the C_β–H···M unit. A major advantage of the new model is its apparent ability to *prioritize* the importance of competing factors in the development or inhibition of agostic interaction. This endows it, at least in principle, with a predictive capability beyond the reach of the valence-bond approach.

4. Conclusions

In the preceding sections we have outlined the case histories of some molecules that have been found to be at variance with the predictions of the simple VSEPR model in the equilibrium structures they assume in their electronic ground states. Most of these molecules are characterized by a metal atom hub whose electron core, while polarizable, would be expected to function as no more than a spectator to stereochemical choice.

Section 2 has concentrated particularly on alkyl derivatives of d^0 transition metals where the skeletal geometries are found to differ in varying degrees from those of analogous derivatives of Main Group elements. For example, the D_{3h} geometry of the WC_6 framework in WMe_6 contrasts starkly with the regular O_h geometry of the TeC_6 framework in $TeMe_6$, and the pattern of bond angles revealed by the skeleton of Me_2TiCl_2 is quite the opposite of that revealed by Me_2SiCl_2. The polarizability of the central atom may very well hold the key to these anomalies. One way of acknowledging this polarizability is to follow Gillespie's lead [4–6,23] of considering the potential of bonding electron pairs to induce concentrations of

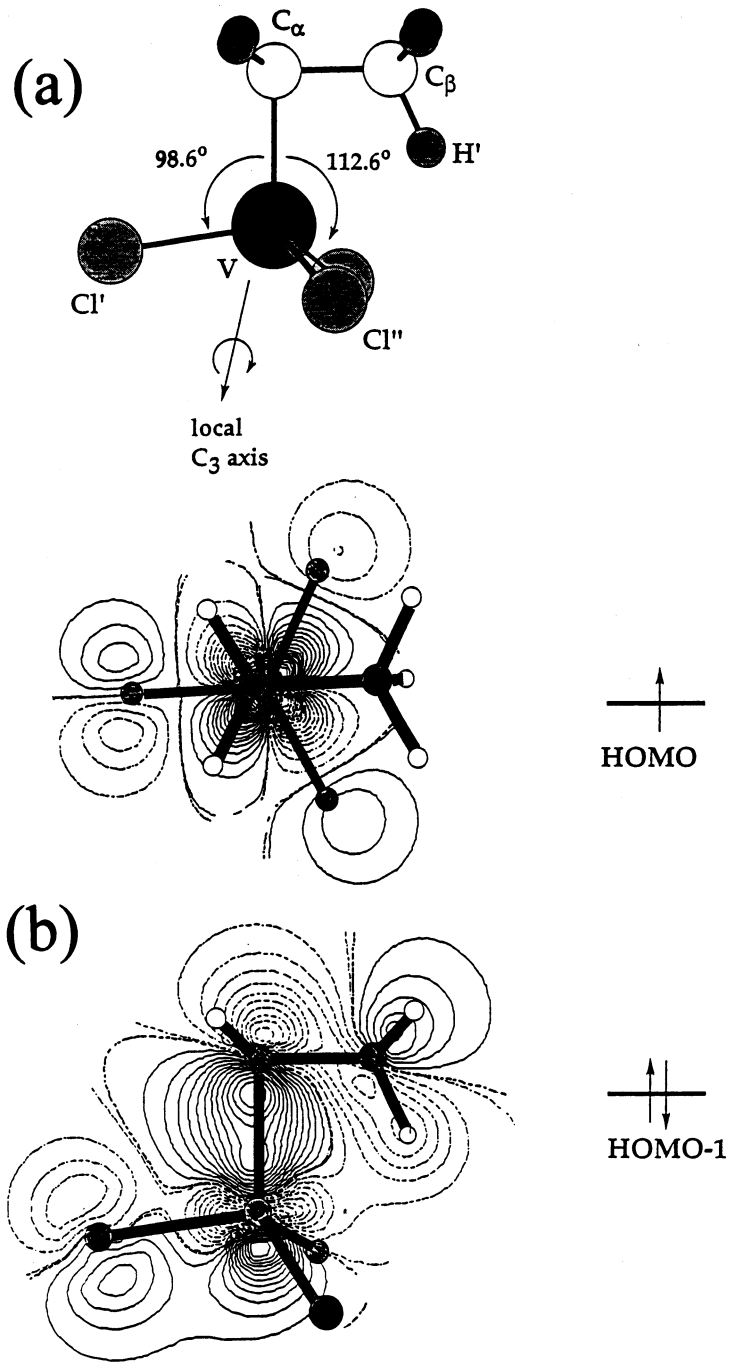

Fig. 12. (a) Coordination geometry of the elipsed (agostic) conformer of $EtVCl_3$. (b) Contour maps of the frontier MOs for $EtVCl_3$: the HOMO contributes to a weakening of the V–Cl bonds and a widening of the $C_\alpha VCl''$ valence angles, and hence assists in the development of a β-agostic interaction. Reproduced with permission from Ref. [61].

charge in the electron core; each such concentration is diametrically opposed to the bond associated with the electron pair inducing it and increases as that bond takes on more covalent character. Alternatively, the rôle of polarizability can be viewed in simple molecular orbital terms as a closing of the energy gap between occupied and unoccupied frontier orbitals, thereby facilitating geometric change as induced by a second-order Jahn–Teller event [49].

Section 3 is concerned with some problems of secondary bonding, and specifically with the so-called agostic interaction that can develop between an alkyl ligand and the d^0 transition metal center to which it is linked, apparently via a conventionl σ-bond. Detailed consideration of ethyltrichlorotitanium, $EtTiCl_3$, highlights the dramatic change in both conformation and geometry of the $Ti–CH_2–CH_3$ fragment brought about by complexation with the diphosphine $Me_2PCH_2CH_2PMe_2$ (dmpe). The interaction responsible for this change appears to involve a delocalization of the $Ti–C_\alpha$ bonding electrons so that the ethyl group assumes a semi-η^2 mode of coordination, and is accommodated partly by the unusual pliability of the $Ti–CH_2–CH_3$ skeleton, and partly by the loosening of the ligand environment as a result of complexation. The experience of $EtTiCl_3$(dmpe) emphasizes the potential significance of secondary intramolecular bonding as a stereochemical influence, but one that is not easily encompassed by the VSEPR model, the virtues of which lie in its very simplicity and comparative freedom from demarcation.

Acknowledgements

We are indebted to three co-workers who have collaborated with us over several years on aspects of our research described in Sections 2 and 3 of this review. Professor Arne Haaland (University of Oslo) and Dr Wolfgang Scherer (Technical University, Munich) have provided excellent input, facilities and support for the electron diffraction and quantum chemical studies, and have shared a common interest in our study of small, reactive organometallic molecules and their relevance to theories of structure and bonding. Professor Donald McKean (University of Edinburgh) has provided an invaluable input to the analysis of the vibrational spectra of these molecules, and has assisted greatly in the extraction of the maximum amount of information from the data. We are grateful also to Dr Fred Armitage (King's College London) for reading the manuscript prior to submission, and for helpful comments and suggestions.

References

[1] N.V. Sidgwick, H.M. Powell, Proc. R. Soc. London A 176 (1940) 153.
[2] R.J. Gillespie, R.S. Nyholm, Quart. Rev. Chem. Soc. 11 (1957) 339.
[3] (a) R.J. Gillespie, J. Chem. Educ. 40 (1963) 295. (b) R.J. Gillespie, Angew. Chem. Int. Ed. Engl. 6 (1967) 819.
[4] R.J. Gillespie, Chem. Soc. Rev. 21 (1992) 59.
[5] R.J. Gillespie, Molecular Geometry, Van Nostrand Reinhold, London, 1972.

[6] R.J. Gillespie, I. Hargittai, The VSEPR Model of Molecular Geometry, Allyn and Bacon, Boston, 1991; Prentice Hall International, London, 1991.
[7] See, for example: (a) L.S. Bartell, Inorg. Chem. 5 (1966) 1635. (b) J.N. Murrell, S.F.A. Kettle, J.M. Tedder, The Chemical Bond, second ed., Wiley, Chichester, 1985, p. 145.
[8] (a) J.K. Burdett, Molecular Shapes, Wiley, New York, 1980, p. 38. (b) J.K. Burdett, Chemical Bonds: a Dialog, Wiley, Chichester, 1997, p. 155.
[9] U. Kaldor, J. Chem. Phys. 46 (1967) 1981.
[10] See, for example: (a) R.F.W. Bader, P.J. MacDougall, C.D.H. Lau, J. Am. Chem. Soc. 106 (1984) 1594. (b) R.F.W. Bader, R.J. Gillespie, P.J. MacDougall, J. Am. Chem. Soc. 110 (1988) 7320.
[11] (a) K.W. Hansen, L.S. Bartell, Inorg. Chem. 4 (1965) 1777. (b) H. Yow, L.S. Bartell, J. Mol. Struct. 15 (1973) 209.
[12] (a) A.J. Downs, G.S. McGrady, E.A. Barnfield, D.W.H. Rankin, J. Chem. Soc. Dalton Trans. (1989) 545. (b) D. Christen, J. Kadel, A. Liedtke, R. Minkwitz, H. Oberhammer, J. Chem. Phys. 93 (1989) 6672. (c) H. Beckers, J. Breidung, H. Bürger, R. Kuna, A. Rahner, W. Schneider, W. Thiel, J. Chem. Phys. 93 (1990) 4603.
[13] R.H. Crabtree, P.E.M. Siegbahn, O. Eisenstein, A.L. Rheingold, T.F. Koetzle, Acc. Chem. Res. 29 (1996) 348.
[14] See, for example: M. Müller, V.C. Williams, L.H. Doerrer, M.A. Leech, S.A. Mason, M.L.H. Green, K. Prout, Inorg. Chem. 37 (1998) 1315.
[15] See, for example: (a) P.L.A. Popelier, G. Logothetis, J. Organomet. Chem. 555 (1998) 101. (b) P. Macchi, D.M. Proserpio, A. Sironi, J. Am. Chem. Soc. 120 (1998) 1447. (c) B.N. Figgis, A.N. Sobolev, D.M. Young, A.J. Schultz, P.A. Reynolds, J. Am. Chem. Soc. 120 (1998) 8715. (d) Y.A. Abramov, L. Brammer, W.T. Klooster, R. Bullock, Inorg. Chem. 37 (1998) 6317.
[16] See, for example: (a) A.J. Blake, P.T. Brain, H. McNab, J. Miller, C.A. Morrison, S. Parsons, D.W.H. Rankin, H.E. Robertson, B.A. Smart, J. Phys. Chem. 100 (1996) 12280. (b) P.T. Brain, H.E. Brown, A.J. Downs, T.M. Greene, E. Johnsen, S. Parsons, D.W.H. Rankin, B.A. Smart, C.Y. Tang, J. Chem. Soc. Dalton Trans. (1998) 3685.
[17] (a) D.C. McKean, Chem. Soc. Rev. 7 (1978) 399. (b) D.C. McKean, Croat. Chem. Acta 61 (1988) 447. (c) D.C. McKean, Int. J. Chem. Kinet. 21 (1989) 445.
[18] G.S. McGrady, A.J. Downs, N.C. Bednall, D.C. McKean, W. Thiel, V. Jonas, G. Frenking, W. Scherer, J. Phys. Chem. A. 101 (1997) 1951 and references cited therein.
[19] R.G. Parr, W. Yang, Density Functional Theory of Atoms and Molecules, Oxford University Press, New York, 1989.
[20] L. Wharton, R.A. Berg, W. Klemperer, J. Chem. Phys. 39 (1963) 2023.
[21] See, for example: V. Calder, D.E. Mann, K.S. Shishadri, M. Allavena, D. White, J. Chem. Phys. 51 (1969) 2093.
[22] M. Hargittai, in: I. Hargittai, M. Hargittai (Eds.), Stereochemical Applications of Gas Phase Electron Diffraction, vol. B, VCH, New York, 1988, p. 383.
[23] R.J. Gillespie, I. Bytheway, T.-H. Tang, R.F.W. Bader, Inorg. Chem. 35 (1996) 3954 (and refs. 1 and 2 therein).
[24] A. Almenningen, S. Samdal, D. Christen, J. Mol. Struct. 48 (1978) 69.
[25] R.J. French, L. Hedberg, K. Hedberg, G.L. Gard, B.M. Johnson, Inorg. Chem. 22 (1983) 892.
[26] S.D. Brown, P.J. Green, G.L. Gard, J. Fluorine Chem. 5 (1975) 203.
[27] P.M. Morse, G.S. Girolami, J. Am. Chem. Soc. 121 (1989) 4114.
[28] A. Haaland, A. Hammel, K. Rypdal, H.V. Volden, J. Am. Chem. Soc. 112 (1990) 4547.
[29] C. Pulham, A. Haaland, A. Hammel, K. Rypdal, H.P. Verne, H.V. Volden, Angew. Chem. Int. Ed. Engl. 31 (1992) 1464.
[30] (a) P.J. Wheatley, J. Chem. Soc. (1964) 3718. (b) A.L. Beauchamp, M.J. Bennett, F.A. Cotton, J. Am. Chem. Soc. 90 (1968) 6675.
[31] (a) A.J. Shortland, G. Wilkinson, J. Chem. Soc. Dalton Trans. (1973) 872. (b) A.L. Calyer, G.J. Wilkinson, J. Chem. Soc. Dalton Trans. (1976) 2235.
[32] V. Pfennig, K. Seppelt, Science 271 (1996) 626.
[33] S. Kleinhenz, V. Pfennig, K. Seppelt, Chem. Eur. J. 4 (1998) 1687.
[34] V. Pfennig, N. Robertson, K. Seppelt, Angew. Chem. Int. Ed. Engl. 36 (1997) 1350.

[35] P. Briant, J. Green, A. Haaland, H. Møllendal, K. Rypdal, J. Tremmel, J. Am. Chem. Soc. 111 (1989) 3434.
[36] G.S. McGrady, A.J. Downs, D.C. McKean, A. Haaland, W. Scherer, H.P. Verne, H.V. Volden, Inorg. Chem. 35 (1996) 4713.
[37] G.S. McGrady, A.J. Downs, A. Haaland, H.P. Verne, H.V. Volden, W. Scherer, unpublished results.
[38] W.A. Herrmann, P. Kiprof, K. Rypdal, J. Tremmel, R. Blom, R. Alberto, J. Behm, R.W. Albach, H. Bock, B. Solouki, J. Mink, D. Lichtenberger, N.E. Gruhn, J. Am. Chem. Soc. 113 (1991) 6527.
[39] A. Haaland, W. Scherer, H.V. Volden, H.P. Verne, O. Groppen, G.S. McGrady, A.J. Downs, G. Dierker, W.A. Herrmann, P.W. Roesky, M.R. Geisberger, Organometallics, in press.
[40] G. Vacek, V.S. Mastryukov, H.F. Schaefer, III, J. Phys. Chem. 98 (1994) 11337.
[41] C.N. Field, J.C. Green. N. Kaltsoyannis, G.S. McGrady, A.N. Moody, M. Siggel, M. DeSimone, J. Chem. Soc. Dalton Trans. (1997) 213.
[42] (a) R.G. Cavell, D.P. Poulin, K.I. The, A.J. Tomlinson, J. Chem. Soc. Chem. Commun. (1974) 19. (b) R.G. Cavell, J.A. Gibson, K.I. The, J. Am. Chem. Soc. 99 (1977) 7841.
[43] (a) R.F.W. Bader, Atoms in Molecules: A Quantum Theory, Oxford University Press, Oxford, UK, 1990. (b) R.F.W. Bader, R.J. Gillespie, P.J. MacDougall, J. Am. Chem. Soc. 110 (1988) 7329.
[44] I. Bytheway, R.J. Gillespie, T.-H. Tang, R.F.W. Bader, Inorg. Chem. 34 (1995) 2407.
[45] R. Hoffmann, J.M. Howell, A.R. Rossi, J. Am. Chem. Soc. 98 (1976) 2484.
[46] A. Demolliens, Y. Jean, O. Eisenstein, Organometallics 5 (1986) 1457.
[47] S.K. Kang, H. Tang, T.A. Albright, J. Am. Chem. Soc. 115 (1993) 1971.
[48] M. Kaupp, J. Am. Chem. Soc. 118 (1996) 3018; Chem. Eur. J. 4 (1998) 1678.
[49] J.K. Burdett, Molecular Shapes, Wiley, New York, 1980, pp. 68ff, 175, 181.
[50] (a) C.R. Landis, T.K. Firman, D.M. Root, T. Cleveland, J. Am. Chem. Soc. 120 (1998) 1842. (b) C.R. Landis, T. Cleveland, T.K. Firman, ibid, 120 (1998) 2641.
[51] (a) G.J. Kubas, Acc. Chem. Res. 21 (1988) 120. (b) D.M. Heinekey, W.J. Oldham, Jr., Chem. Rev. 93 (1993) 913.
[52] (a) H.A. Bent, J. Chem. Ed. 37 (1960) 616. (b) H.A. Bent, Chem. Rev. 61 (1961) 275.
[53] V. Jonas, C. Boehme, G. Frenking, Inorg. Chem. 35 (1996) 2097.
[54] (a) M. Brookhart, M.L.H. Green, J. Organomet. Chem. 250 (1983) 395. (b) M. Brookhart, M.L.H. Green, L.-L. Wong, Prog. Inorg. Chem. 36 (1988) 1. (c) Z. Dawoodi, M.L.H. Green, V.S.B. Mtetwa, K. Prout, A.J. Schultz, J.M. Williams, T.F. Koetzle, J. Chem. Soc. Dalton Trans. (1986) 1629.
[55] T. Ziegler, Can. J. Chem. 73 (1995) 743.
[56] H.H. Brintzinger, D. Fischer, R. Mülhaupt, B. Rieger, R.M. Waymouth, Angew. Chem. Int. Ed. Engl. 34 (1995) 1143.
[57] (a) J.J. Schneider, Acc. Chem. Res. 35 (1996) 1068. (b) R.H. Crabtree, Angew. Chem. Int. Ed. Engl. 22 (1993) 789.
[58] (a) R.H. Crabtree, Chem. Rev. 85 (1985) 245. (b) R.G. Bergman, Science, 233 (1984) 902. (c) R.H. Crabtree, D.G. Hamilton, Adv. Organomet. Chem. 28 (1988) 299. (d) W.D. Jones, F.J. Feher, Acc. Chem. Res. 22 (1989) 99.
[59] W. Scherer, T. Priermeier, A. Haaland, H.V. Volden, G.S. McGrady, A.J. Downs, R. Boese, D. Bläser, Organometallics 17 (1998) 4406.
[60] A.J. Downs, C.R. Pulham, Adv. Inorg. Chem. 41 (1994) 171.
[61] A. Haaland, W. Scherer, K. Ruud, G.S. McGrady, A.J. Downs, O. Swang, J. Am. Chem. Soc. 120 (1998) 3762.
[62] (a) G.S. McGrady, A.J. Downs, A. Haaland, W. Scherer, D.C. McKean, J. Chem. Soc. Chem. Commun. (1997) 1547. (b) D.C. McKean, G.S. McGrady, A.J. Downs, W. Scherer, A. Haaland, J. Phys. Chem. A. submitted for publication.
[63] R.B. Calvert, J.R. Shapley, J. Am. Chem. Soc. 100 (1978) 7726.
[64] (a) M.LH. Green, A.K. Hughes, N.A. Popham, A.H.H. Stephens, L.-L. Wong, J. Chem. Soc. Dalton Trans. (1992) 3077. (b) D.C. Maus, V. Copié, B. Sun, J.M. Griffiths, R.G. Griffin, S. Luo, R.R. Schrock, A.H. Liu, S.W. Seidel, W.M. Davis, A. Grohmann, J. Am. Chem. Soc. 118 (1996) 5665.
[65] W. Scherer, W. Hieringer, M. Spiegler, P. Sirsch, G.S. McGrady, A.J. Downs, A. Haaland, B. Pedersen, J. Chem. Soc. Chem. Commun. (1998) 2471.